Published in final edited form as:
Pharm Res. 2009 May ; 26(5): 1217–1225. doi:10.1007/s11095-008-9729-6.

Solubility, Stability, Physicochemical Characteristics and *In Vitro* Ocular Tissue Permeability of Hesperidin: a Natural Bioflavonoid

Soumyajit Majumdar[1,2,#] and **Ramesh Srirangam**[1]

1 *Department of Pharmaceutics, School of Pharmacy, The University of Mississippi, University, MS 38677*

2 *Research Institute of Pharmaceutical Sciences, The University of Mississippi, University, MS 38677*

Abstract

Purpose—Hesperidin holds potential in treating age-related macular degeneration, cataract and diabetic retinopathy. The aim of this study, constituting the first step towards efficient ocular delivery of hesperidin, was to determine its physicochemical properties and *in vitro* ocular tissue permeability.

Methods—pH dependent aqueous solubility and stability were investigated following standard protocols. Permeability of hesperidin across excised rabbit cornea, sclera, and sclera plus retinal pigmented epithelium (RPE) was determined using a side-bi-side diffusion apparatus.

Results—Hesperidin demonstrated poor, pH independent, aqueous solubility. Solubility improved dramatically in the presence of 2-hydroxypropyl-beta-cyclodextrin (HP-β-CD) and the results supported 1:1 complex formation. Solutions were stable in the pH and temperature (25, 40°C) conditions tested, except for samples stored at pH 9. Transcorneal permeability in the apical-basal and basal-apical directions was $1.11\pm0.86\times10^{-6}$ and $1.16\pm0.05\times10^{-6}$ cm/s, respectively. The scleral tissue was more permeable ($10.2\pm2.1\times10^{-6}$cm/s). However, permeability across sclera/choroid/RPE in the sclera to retina and retina to sclera direction was $0.82\pm0.69\times10^{-6}$, $1.52\pm0.78\times10^{-6}$ cm/s, respectively, demonstrating the barrier properties of the RPE.

Conclusion—Our results suggest that stable ophthalmic solutions of hesperidin can be prepared and that hesperidin can efficiently permeate across the corneal tissue. Further investigation into its penetration into the back-of-the eye ocular tissues is warranted.

INTRODUCTION

Recently, it has been reported that among non-institutionalized American adults, 18 years or older, prevalence of visual impairment is 9.3%, including 0.3% with blindness (1). The major eye diseases like cataract, glaucoma, macular degeneration and diabetic retinopathy, are supposedly the leading causes. Pathophysiology of diabetic retinopathy involves the process of physiological or pathological angiogenesis. Oxidative damage to the retinal neuronal cells as a result of free radical generation, a complication associated with diabetes, is considered to be a principal factor responsible for the initiation and progression of diabetic retinopathy (2). Decreased retinal blood supply, as a consequence of long term diabetes is another major contributor to the progression of this disease. In patients with diabetes, proliferative diabetic

#Author for correspondence: Soumyajit Majumdar, 111 Faser Hall, Department of Pharmaceutics, School of Pharmacy, The University of Mississippi, University, MS 38677; Tel: (662)-915 3793; Fax: (662)-915-1177; E-mail: majumso@olemiss.edu.

This article has been published in Pharmaceutical Research. The original article is available at http://www.springerlink.com/content/g7633q2816316074/

retinopathy is the neovascular result wherein ischemia induced angiogenesis on the surface of the retina, and into the vitreous, is postulated to occur. Increased permeability in these vessels can lead to diabetic macular edema, the major factor responsible for vision loss (2).

Hesperidin (hesperetin 7-rutinoside) is a flavanone glycoside, comprising of an aglycone, hesperetin, and an attached disaccharide, rutinose. The structures of hesperidin and hesperetin are illustrated in Figure 1. Hesperidin is abundantly found in citrus fruits (family *Rutaceae*) and has also been reported to occur in many plants other than Citrus, such as in genera *Fabaceae, Betulaceae, Laminaseae* and *Papilionaceae.* What makes hesperidin, and hesperetin, particularly attractive for the treatment of diabetic retinopathy or macular degeneration is their potential effect on ocular blood flow and vascular permeability, two important factors leading to the initiation and progression of diabetic retinopathy. It has been demonstrated that these compounds can support retinal function recovery subsequent to retinal ischemia (3). Hesperidin's effect on ocular blood vessels has not been studied. However, this compound was initially referred to as 'Vitamin P' to indicate that it could decrease capillary permeability and fragility, although subsequently the term vitamin P has been discontinued (4). Literature reports suggest that hesperidin can prevent microvascular leakage by virtue of its vasoprotective action through the inhibition of the enzyme hyaluronidase which is reported to regulate the permeability of capillary walls and supporting tissues (5). Additionally, it has been demonstrated that hesperidin can decrease blood cell and platelet aggregation, believed to be beneficial in cases of capillary permeability and fragility (4).

Besides their effect on vascular permeability and ocular blood flow, both hesperidin and hesperetin demonstrate strong antioxidant properties (6). This antioxidant activity is through their ability to quench oxidative radical chain reactions (capable of oxidizing and nitrating cellular proteins, nucleic acids, and lipids), and can thus help preserve neuronal health. Hesperidin also exhibits significant anti-inflammatory activity by modulating the prostaglandin synthesis and COX-2 gene expression pathways (7). Ayalasomayajula *et al.*(8) reported that, in diabetic rat retina, up-regulation of COX-2 is responsible for production of prostaglandin E2, a pro-angiogenic factor implicated in vascular permeability and leakage. This prostaglandin up-regulation was inhibited by celecoxib (8), a selective COX-2 inhibitor.

Hesperidin has been reported to possess analgesic (9), hypolipidemic (10), anti-hypertensive and diuretic activity (11). Another potential therapeutic application of hesperidin is its anticancer activity mediated through the suppression of cell proliferation (12,13). Thus, both hesperidin and its metabolite hesperetin, appear to be capable of modulating multiple pathways (Fig. 2) identified in the genesis and progression of diabetic retinopathy and diabetic macular edema. It can also be used in other ocular diseases because of its varied pharmacological actions.

Currently hesperidin is used as a dietary supplement for improving blood flow and for its vasoprotective properties, and is available as an oral dosage form. Ameer *et al.* (14) reported that following oral administration, hesperidin is absorbed across the gastrointestinal tract, but cumulative urinary recovery indicates low bioavailability (<25%). Several factors limit oral bioavailability of hesperidin, including poor water solubility and precipitation in an acidic environment (15). Moreover, hesperidin and hesperetin are substrates of the intestinal efflux protein, P-glycoprotein (P-pg), (16–18) and intestinal and hepatic drug metabolizing enzymes CYP450 (19). These factors, acting together, severely restrict systemic bioavailability of the orally administered drug. Furthermore, hesperidin possesses poor transmembrane permeability and is believed to be absorbed primarily by the paracellular pathway (20,21). Thus intestinal tight junction proteins would limit intestinal absorption. Additionally, reports indicate that hesperidin needs to be converted to hesperetin, by the beta-glycosidases secreted by the intestinal flora (22), for absorption to occur.

Over and above all the barriers to oral bioavailability, in order to exert a therapeutic effect in diabetic retinopathy, hesperidin must penetrate into the neural retina from the systemic circulation. For this, it needs to permeate across the blood-retinal barrier (BRB), formed by retinal pigmented epithelium (RPE) and endothelial cells of retinal blood vessels. The diffusion limiting capabilities of the BRB has been well established for both hydrophilic (limited by tight junctions) as well as lipophilic (through efflux mechanism) compounds. Thus, following oral administration very little, if any, amounts of hesperidin can reach the neural retina.

The long term goal of this project is to achieve therapeutically optimal hesperidin concentrations at the target site, i.e. posterior segment of the eye. Considering the barriers encountered in oral/systemic administration, topical instillation may be an attractive alternative for producing therapeutic hesperidin levels at the active site. Some other possible routes/modes of administration for achieving higher drug concentrations in the retina include intravitreal injection and implants. However, these are invasive techniques and are associated with side-effects such as retinal detachment and endophthalmitis.

For a topically administered drug, penetration into the posterior chamber tissues, such as the RPE, may be through corneal or noncorneal routes. Transcorneal absorption represents the major route of penetration for most therapeutic agents. However, several studies demonstrate that the noncorneal route is also a significant route, wherein the drug molecule is supposed to penetrate into the intraocular tissues via diffusion across the conjunctiva and sclera (23).

Thus, the objective of this project, constituting the first step towards efficient ocular delivery of hesperidin, was to determine hesperidin's solubility, stability, physicochemical properties and *in vitro* permeability across the ocular tissues-cornea, sclera and RPE.

MATERIALS AND METHODS

Materials

Hesperidin, hesperetin and 2-hydroxypropyl beta cyclodextrin (HP-β-CD) (1300 MW 0.6 substitution) were purchased from Sigma-Aldrich (St.Louis, MO, USA). [^{14}C]mannitol was purchased from American Radiolabelled Chemicals Inc. (St. Louis, MO, USA) and [^{3}H] diazepam was obtained from PerkinElmer Life and Analytical Sciences (Boston, MA, USA). All other chemicals and solvents were obtained from Fisher Scientific, USA.

Ocular tissues

Ocular tissues were isolated from euthanized adult male New Zealand albino rabbits weighing between 2–2.5kg (Myrtle's Rabbitry, Thompson Station, TN, USA). Experiments using rabbits conformed to the tenets of the Association for Research in Vision and Ophthalmology statement on the Use of Animals in Ophthalmic and Vision Research. Each experiment was conducted at least in quadruplicates.

Solubility Studies

Aqueous solubility of hesperidin was determined following standard shake flask method wherein excess quantity of drug was added to 5mL of solvent in a tightly capped glass vial. To achieve uniform mixing, samples were constantly agitated at 75rpm at room temperature (25° C) for 24h in a reciprocating water bath (Fisher Scientific, USA). At the end of 24h, samples were centrifuged (AccuSpin 17R, Fisher Scientific, USA) and the supernatant was analyzed for drug content. Solubility was determined in water and in buffers with pH values ranging between 1.2 and 9. Additionally, effect of surfactants and HP-β-CD on the solubility of hesperidin, was also evaluated. HP-β-CD concentrations used for the phase solubility studies were 1, 2.5, 5, 7.5, 10, 15 and 20%w/v in water.

Differential Scanning Calorimetry (DSC) Studies

DSC analysis of hesperidin, HP-β-CD, physical mixture of hesperidin and HP-β-CD (1:1 molar ratio) and the complex were carried out using a Diamond Differential Scanning Calorimeter (PerkinElmer Life and Analytical Sciences, Shelton, CT, USA). Samples, 2–3 mg, were heated in a hermetically sealed aluminium pans at a heating rate of 10 °C/min (25–280 °C range) under a nitrogen atmosphere (flow rate 20mL/min). An empty aluminium pan was used as the reference.

Fourier Transform Infrared Spectroscopy (FTIR) Studies

FTIR spectra were obtained using a Perkin Elmer FTIR spectrometer (PerkinElmer Life and Analytical Sciences, Shelton, CT, USA). Samples were mixed with dry crystalline KBr in a 1:100 (sample: KBr) ratio and pellets were prepared. A spectrum was collected for each sample within the wave number region 4000–400 cm^{-1}.

LogP

Predicted value of LogP was obtained using the ACD/I-Lab web service (ACD/LogP 8.02).

pH Stability

Solution stability of hesperidin was determined at various pH (1.2, 3, 5, 7.4, and 9) and temperature (25 and 40°C) conditions. Buffers were prepared according to USP. Stability studies were initiated with the addition of 25μL of a 1mg/mL hesperidin stock solution to 5mL of the respective buffer previously equilibrated to either 25 or 40°C. Aliquots (200μL) were collected at 0, 0.5, 1, 2, 3, 4, 5, 6, 7, 14, 30 and 60 days and were stored at −80°C until further analysis. Samples were analyzed using HPLC technique as described under the analytical method section.

Stability in Ocular Tissue Homogenates

Ocular tissues isolated from New Zealand albino rabbits were used for the metabolism studies. Animals were euthanized with an overdose of pentobarbital administered through the marginal ear vein. Eyes were enucleated immediately and washed with ice-cold Dulbecco's Phosphate Buffered Saline (DPBS pH 7.4) to remove traces of blood. Vitreous humor was collected through an incision in the sclera. Sclera was isolated with the retinal pigmented epithelium (RPE) attached. The RPE/choroid section was then carefully separated from underlying sclera. This procedure takes approximately 10–15 min. The pooled RPE/choroid tissue was homogenized (TISSUMISER, Fisher Scientific, USA) in 2mL ice-cold Isotonic Phosphate Buffer Saline (IPBS), pH 7.4, and then centrifuged at 4°C (accuSpin 17R, Fisher Scientific, USA). Supernatant was collected and estimated for total protein content by the method of Bradford (Sigma-Aldrich, USA) (24). Final protein concentration was adjusted to 1mg/mL by diluting with IPBS and used for the hydrolysis studies. Vitreous humor was used as such without any dilution or homogenization.

Reactions were initiated by adding 20μL of drug solution (1mg/mL) to 2mL of the supernatant. The reactions were carried out in a water bath at 37°C. Samples (100μL) were withdrawn at predetermined time intervals and the enzymatic degradation process was arrested with the addition of an equal volume of ice-cold methanol:acetonitrile mixture (60:40). Rate of hydrolysis in IPBS pH 7.4 at 37°C was used as a control. Samples were analyzed using an HPLC technique as described under the analytical method section. Experiments were carried out in triplicate.

Corneal Permeation Studies

Permeation of hesperidin was studied using a side-bi-side diffusion apparatus (PermeGear, Inc.). Conreas isolated from New Zealand Albino male rabbits were used for these studies. Rabbits were euthanized, and eyes were collected as described earlier. Cornea was isolated with a ring of sclera around it, which helps in mounting between diffusion cells. Corneas were washed in DPBS and mounted on the side-bi-side diffusion apparatus (standard 9 mm cells were used) (Fig. 3A) with the epithelial side facing the donor cell for apical to basolateral transport (A-B), and with the endothelial side facing the donor cell for basolateral to apical transport (B-A). Temperature of the cells was maintained at 34°C with the help of a circulating water bath. In all cases, 3mL of transport buffer (DPBS containing 5% HP-β-CD) or drug solution (150μM of hesperidin in DPBS with 5% HP-β-CD) was added to the apical side of the cornea while 3.2mL was added to the basal side, to maintain the natural hydrostatic pressure. Aliquots (200μL) were removed at predetermined time points (15, 30, 45, 60, 90, 120, 150 and 180min) from the receiver side and the volume withdrawn was replaced with an equal volume of transport buffer. Samples were stored at −80°C until further analysis.

Similar procedures were followed to determine transcorneal permeability of [^{14}C]mannitol (55mCi/mmol) and [^{3}H]diazepam (70Ci/mmol), both at 0.5 μCi/mL concentration. Five milliliters of scintillation cocktail (Fisher Scientific, USA) was added to each sample and radioactivity was measured using Liquid Scintillation Analyzer (PerkinElmer Life and Analytical Sciences, Model Tri-Carb 2900TR, Shelton, CT, USA).

Permeation across Sclera and Retinal Pigmented Epithelium (RPE)

Transscleral permeation studies were carried out using the 5mm diameter Valia-Chein side-bi-side diffusion cells from PermeGear, Inc (Fig. 3B). After carefully isolating sclera alone, or sclera with RPE/choroid, the tissues were mounted in a manner such that outer surface of the sclera, known as the episclera, faced the donor side (Fig. 3B; half-cell a) and the inner side of sclera, or the RPE side, faced the receiver chamber (Fig. 3B half-cell b) for the transport studies in the sclera to choroid/RPE direction (S to R direction). Donor solution was added to the RPE/choroid side (Fig. 3B half-cell b) for transport in the RPE/choroid to scleral direction (R to S direction). Temperature of the cells was maintained at 37°C with the help of a circulating water bath. 150μM of hesperidin in DPBS with 5% HP-β-CD was placed in donor chamber and DPBS with 5% HP-β-CD was placed in receiver chamber. Aliquots (200μL) were removed at predetermined time points (15, 30, 45, 60, 90, 120, 150 and 180min) from the receiver side and replaced with an equal volume of transport buffer. Samples were stored at −80°C until further analysis.

Similar procedures were followed to determine permeability of [^{14}C]mannitol (55mCi/mmol) and [^{3}H]diazepam (70Ci/mmol), both at 0.5 μCi/mL concentration, across sclera/choroid/RPE. Five milliliters of scintillation cocktail (Fisher Scientific, USA) was added to each sample and radioactivity was measured using Liquid Scintillation Analyzer.

Analytical Method

Hesperidin content in samples collected from the solubility, stability and permeability studies was estimated using an analytical method based on reversed phase HPLC. An HPLC system equipped with Waters 600 pump controller, 2470 dual wavelength UV detector, refrigerated 717 plus auto-sampler and Agilent 3394B integrator was used. The detector was operated at 284nm. Mobile phase consisted of 20mM monobasic potassium phosphate (pH adjusted to 2.5 with orthophosphoric acid) and acetonitrile in a ratio of 75:25 and flow rate was maintained at 1mL/min. A Waters Symmetry Shield C18 column was used.

Analytical method for the determination of hesperetin content was also developed. The method for hesperetin was similar to that for hesperidin, except for the mobile phase, which, in this case, was a 50:50 mixture of acetonitrile and 20mM monobasic potassium phosphate (pH adjusted to 2.5 with orthophosphoric acid).

DATA ANALYSIS

Cumulative amount (M_n) transported was calculated using Equation 1 and Steady state (SS) fluxes ($\mu g/min/cm^2$) were determined from the slope of the cumulative amount of drug transported vs. time graph and expressed as per unit of surface area as described by Equation 2.

$$M_n = V_r C_{r(n)} + \sum_{x=1}^{x=n} V_{S(x-1)} C_{r(x-1)} \quad \text{(Eq. 1)}$$

$$\text{Flux}(J) = \frac{(dM/dt)}{A} \quad \text{(Eq. 2)}$$

Where, M_n is the cumulative amount of the drug in the receiver chamber at n^{th} sampling time point (n=1, 2, 3, 4, 5, 6, 7 and 8 corresponding to 15, 30, 45, 60, 90, 120, 150 and 180min sampling points), V_r is the volume of the medium in the receiver chamber, V_S is the volume of the sample withdrawn at the n^{th} time point, $C_{r(n)}$ is the concentration of the drug in the receiver chamber medium at n^{th} time point, A is the surface area of the tissue exposed to the permeant (surface area of cornea and sclera/RPE exposed is 0.636 and 0.192 cm^2, respectively). Note that when n=1, the second part of the right hand side of Equation 1 becomes zero since concentration in the receiver chamber, C_r, is zero at time zero.

Membrane permeability (cm/s) values were determined by normalizing the steady state fluxes to the donor concentration, C_d according to Equation (3).

$$\text{Permeability } (P_{app}) = \text{Flux}/C_d \quad \text{(Eq. 3)}$$

STATISTICAL ANALYSIS

All experiments were carried out at least in triplicate. Unpaired t-test and ANOVA was used for statistical analysis. In all the cases a p value less than 0.05 was considered to denote statistically significant difference.

RESULTS AND DISCUSSION

Diabetic retinopathy and macular edema are serious sight threatening conditions. While involvement of several mechanisms in the pathogenesis of this disease has been suggested, a drug candidate capable of blocking multiple pathways remains to be identified, as yet. Current treatment options, apart from controlling blood glucose and lipid levels, include corticosteroids, anti-vascular endothelial growth factor, laser photocoagulation, and vitrectomy. However, long term treatment with these drugs is associated with toxicity and corticosteroids may lead to cataract formation and increased intraocular pressure (25). Hesperidin appears to modulate multiple pathways associated with diabetic retinopathy and

macular edema (Fig. 2) but a suitable ocular delivery mechanism is lacking. In this study, feasibility of developing an ophthalmic solution dosage form of hesperidin was investigated

Solubility is an important factor affecting drug permeability across biological membranes. Solubility of hesperidin in different pH buffers and in water is presented in Table 1. The compound was observed to be very poorly soluble in water and exhibited an aqueous solubility value of 4.95μg/mL (7.5×10^{-6}M) at 25°C. Hesperidin did not demonstrate pH dependent solubility within the pH range of 1.2–9. However, solubility of hesperidin at pH values greater than 9 was significantly higher (data not shown) but was accompanied with degradation. These results are in agreement with the studies reported by Serra *et al.* wherein the pKa of hesperidin has been reported to be 10±0.2 for the two phenolic hydroxyl groups and greater than 11.5 for all of the alcoholic hydroxyl groups (21).

In an attempt to improve hesperidin's aqueous solubility, effect of ethanol, surfactants and HP-β-CD, was evaluated. Ethanol and surfactants such as Tween 80 and TPGS (d-alpha-tocopheryl polyethylene glycol 1000 succinate) were ineffective. However, HP-β-CD markedly improved hesperidin's solubility. Cyclodextrins are a group of cyclic oligosaccharides that have been shown to improve solubility of a multitude of poorly soluble compounds, through the formation of inclusion complexes. Among the different cyclodextrins available, HP-β-CD has been reported to be safe for use in ocular preparations (26,27), even when used at concentrations as high as 45% (28).

A linear increase in aqueous solubility of hesperidin was observed with increasing concentrations of HP-β-CD (Fig. 4 and Table 2) suggesting formation of a 1:1 inclusion complex between hesperidin and HP-β-CD. It is interesting to note that hesperidin's solubility was increased approximately 100-fold in the presence of 20% HP-β-CD. The solubility limit of the complex was not reached within the concentration range of HP-β-CD used in this study. Stoichiometry, binding constant (K) and aqueous saturation solubility (S_0) were determined from a plot of solubility as a function of HP-β-CD concentration using Equation 4, according to the method proposed by Higuchi and Connors. Hesperidin binding constant was calculated to be 625±78 M^{-1} (R^2=0.975±0.023, slope=0.0052±0.0006).

$$K=\frac{\text{Slope}}{S_0(1-\text{Slope})} \qquad \text{(Eq. 4)}$$

Further evidence of the formation of an inclusion complex was obtained from thermal and spectral analysis. The DSC thermograms are presented in Figure 5. DSC scans of pure hesperidin showed an endothermic peak at 259°C, corresponding to the melting point of the compound. Physical mixture of the drug and HP-β-CD, in a 1:1 molar ratio, also exhibited the endothermic peak associated with hesperidin. However, the peak was not observed in the complex, prepared by dissolving both the components in methanol (1:1 molar ratio) followed by evaporation. This suggests molecular encapsulation of drug inside the cyclodextrin cavity. FTIR scans complemented the DSC data (Fig. 6). Hesperidin spectra demonstrate a strong absorption band at 1644 cm^{-1}, corresponding to its carbonyl stretching vibration. This characteristic carbonyl stretching vibration was shifted to 1652 cm^{-1} in the complex and was much broader, suggesting the formation of complex. Thus, chemical, thermal and spectral analysis, taken together, strongly supports the formation of an inclusion complex.

Phase solubility studies pointed towards the formation of the complex in a 1:1 molar ratio, which is consistent with an earlier report by Tommasini *et al.* (29). However, the observed intrinsic solubility of hesperidin (7.5×10^{-6} M) in the current study was less than the value (3.6×10^{-5}M) reported by Tommasini *et al*. Also, the estimated binding constant in the previous

study was $60M^{-1}$. The observed differences, between the earlier report and the current study, with respect to these two parameters, may be attributed to the experiment protocol. While Tommasini *et al.* sonicated the excess drug containing cyclodextrin solution for a period of 15min and then allowed equilibration for a period of 4 days, in the current study sonication was not a part of the protocol and equilibration period allowed was only 24h.

Hesperidin, a flavonoid glycoside, can be converted into its aglycone, hesperetin through chemical or enzymatic processes. Stability studies in aqueous solutions did not demonstrate any decrease in hesperidin content upto 2 months, the final time point tested, in the pH range and temperature conditions employed. The only exception was pH 9 samples. In this case, degradation rate constant and half-lives, at 25 and 40°C were observed to be 0.03 and 0.15 day^{-1}, and, 23 and 4.5 days, respectively (Fig. 7). This signifies that hesperidin may undergo alkaline hydrolysis at higher pH and temperature conditions.

Hesperidin undergoes enzymatic degradation by beta-glucosidases to yield hesperetin. Literature reports suggest that beta-glucosidases are expressed in the ocular tissues, especially in the RPE (30,31). Ideally, one would like to maintain the drug in the unmetabolized form at the target tissue for maximizing therapeutic effect. With respect to hesperidin, however, both hesperidin and its aglycone hesperetin, are pharmacologically active. Even then, it is important to know the rate of generation of hesperetin, from hesperidin, in the ocular tissues as the two compounds would exhibit different pharmacokinetic profiles. For example, hesperetin is more lipophilic than hesperidin and is known to be a much better substrate of the efflux protein P-gp, which is also known to be expressed on the RPE (32). Consequently, conversion of hesperidin to hesperetin may impact therapeutic activity. Taking this into consideration, stability of hesperidin in ocular tissue homogenates was determined. Hesperetin generation, or decrease in hesperidin concentrations, in the homogenates was not observed even after 15h. Further studies investigating generation of hesperetin in the ocular tissues *in vivo*, and their in vivo pharmacokinetic profile following topical and intravitreal administration, are in progress.

Oral hesperidin administration for ocular indications may not be very effective. Local delivery of hesperidin for ocular diseases may prove to be a much more viable option, compared to oral administration. To our knowledge, hitherto, permeability of hesperidin across ocular tissues has not been determined. In this study, ocular tissues isolated from New Zealand albino rabbits, a model widely used for ophthalmic drug delivery studies, were used to evaluate feasibility of penetration of hesperidin into the back-of-the eye following topical administration. The predicted Log P value of hesperidin was determined to be 1.78±0.72 using ACD/I-Lab software, which indicated that the compound is fairly lipophilic. Diffusion studies were carried out for 3h, to determine *in vitro* permeability coefficients across cornea, sclera and sclera/choroid/RPE. Stability studies of hesperidin in aqueous buffered solutions and tissue homogenates demonstrated that drug was stable in these matrices for the entire duration of the diffusion experiments. Since hesperidin demonstrates poor aqueous solubility, 5% HP-β-CD was incorporated in the transport buffer.

Trans-epithelial electrical resistance (TEER) was monitored (Multimeter, Agilent Technologies, USA) throughout the duration of the corneal permeation studies, 3h, to evaluate the integrity of tissue in the presence of 5% HP-β-CD. TEER values for corneas exposed to transport buffers with or without HP-β-CD were found to be $5\pm0.3K\Omega cm^2$ throughout, demonstrating lack of any effect of HP-β-CD on ocular tissue integrity at this concentration. The observed TEER is in agreement with previously reported TEER values for rabbit cornea (33). In addition, diffusion of [^{14}C]mannitol, a paracellular marker, and [^{3}H]diazepam, a transcellular marker, were also evaluated. The mean percent cumulative amount of the [^{14}C] mannitol transported per hour across the cornea remained the same, for the duration of the experiment at 1±0.15. In case of diazepam also, mean percent cumulative amount of [^{3}H]

diazepam transported per hour across the cornea remained steady at 1.62±0.04. These results taken together, demonstrate that integrity and viability of the corneal tissues are maintained during the experimental protocol.

Mean cumulative amount of hesperidin transported across ocular tissues as a function of time is depicted in Figure 8 and the permeability coefficients have been presented in Figure 9. Steady state diffusion was achieved within 5min. Less than 2% decrease in hesperidin concentration in the donor solution was observed during the total time course of the experiments signifying maintenance of sink conditions.

Hesperidin's permeability across the rabbit cornea was $1.11\pm0.86\times10^{-6}$ cm/s consistent with other compounds with similar LogP values (34). Although, P-gp has been reported to play a important role in transcorneal drug absorption (32), corneal permeability of hesperidin in the apical to basolateral (A–B; $1.11\pm0.86\times10^{-6}$ cm/s) and basolateral to apical (B-A; $1.16\pm0.05\times10^{-6}$ cm/s) directions did not differ statistically, indicating lack of involvement of any carrier-mediated process (efflux or influx) in the corneal permeation process, at the concentration studied. These results are consistent with an earlier study by Kobayashi *et al*. (20) with Caco-2 cell monolayers demonstrating similar hesperidin permeability in the A–B and B-A directions. The authors concluded that hesperidin permeates through paracellular route and absence of active transport process. Moreover, hesperidin behaves as a neutral molecule in the pH range of 1–10 (21) indicating lack of involvement of any anion or cation transporters.

Transport studies across sclera and sclera/choroid/RPE were carried out using Valia-Chein cells (PermeGear, Inc. USA). To our knowledge, these cells are being adapted for studying permeability across the RPE for the first time. The scleral tissue tends to fold-up into its natural elliptical shape while mounting on the regular flat face cells. This creates mounting problems, especially the risk of damaging the RPE layer. On the other hand, it is very easy to mount the sclera/choroid/RPE tissue on the Valia-Chein cells. To check the validity of the new experimental set up, acyclovir (ACV) transport across sclera with RPE was carried out from the S to R (sclera to RPE) direction. The observed permeability was 2.5×10^{-6} cm/s. Although there are no prior reports for trans-RPE permeability of ACV, Kansara *et al.* (35) reported that the permeability of ganciclovir (GCV) in the S to R direction was 1.61×10^{-6} cm/s. GCV and ACV are very similar structurally, and with respect to their physicochemical characteristics. Moreover, the permeability of ACV and GCV across the rabbit cornea are reported to be very similar (3.5×10^{-6} and 4.1×10^{-6} cm/s, respectively) (36,37), indicating that their membrane permeation characteristics are also comparable. The close approximation of the permeability of ACV obtained using the Valia-Chien cells with that of GCV in the Franz diffusion cells, indicate that the RPE structure was intact during the experimental protocol. Moreover, The mean percent cumulative amount of [^{14}C]mannitol and [^{3}H]diazepam transported per hour across the sclera/choroid/RPE tissues were 0.1±0.04 and 0.08±0.02, respectively, similar to the values reported by Kansara *et al.* (35). The above results indicate that sclera/choroid/RPE tissue maintains its integrity during the experimental protocol.

Permeability of hesperidin across the sclera alone ($10.2\pm2.1\times10^{-6}$ cm/s) was almost 10-fold higher than that across sclera with RPE (Fig. 8 and 9) and that across the cornea. These results thus substantiate the concept that RPE presents a significant barrier to the transscleral diffusion process following systemic as well as topical administration. However, topical instillation should generate significantly higher concentration gradients across the RPE and thus higher retinal hesperidin concentrations.

The barrier properties of the RPE may be as a result of efflux pump involvement or high lipophilicity of the therapeutic agent. The RPE is reported to express P-gp (32), which can

modulate drug clearance from the vitreous humor. To delineate the role of efflux mechanisms on trans-RPE drug delivery, permeability of hesperidin across RPE in both directions i.e. sclera choroid RPE (S-R) and RPE choroid sclera (R-S) was measured and were found to be 0.82 $\pm 0.68\times10^{-6}$ cm/s and $1.52\pm0.78\times10^{-6}$ cm/s, respectively (Fig. 8 and 9). The difference in permeability in the S-R and R-S directions, under the experimental conditions employed, was statistically insignificant suggesting lack of any efflux mechanism.

In conclusion, results from this study suggest that hesperidin solubility can be markedly improved by complexation with HP-β-CD and that hesperidin exhibits sufficient chemical and enzymatic stability in aqueous solutions and biological matrices, respectively. Additionally, ocular tissue permeation characteristics of hesperidin are not limited by efflux mechanisms. Thus, topical delivery of hesperidin in the form of ophthalmic solutions/suspensions appears feasible. A pH range of 6.5–8.5 is considered to be optimal for ophthalmic forumations. Considering the favorable permeability, solubility and stability profiles, it would be reasonable to formulate hesperidin based ophthalmic solutions at pH 7.4. Further investigation into penetration of hesperidin into the back-of-the eye ocular tissues, following topical and systemic administration is warranted.

Acknowledgements

This project was supported by NIH grant numbers P20RR021929, from the National Center for Research Resources, and EY018426-01 from the National Eye Institute. The content is solely the responsibility of the authors and does not necessarily represent the official views of the National Center for Research Resources or the National Eye Institute, National Institutes of Health.

References

1. Ryskulova A, Turczyn K, Makuc DM, Cotch MF, Klein RJ, Janiszewski R. Self-reported age-related eye diseases and visual impairment in the United States: results of the 2002 national health interview survey. Am J Public Health 2008;98:454–61. [PubMed: 18235074]
2. Wilkinson-Berka JL. Vasoactive factors and diabetic retinopathy: vascular endothelial growth factor, cycoloxygenase-2 and nitric oxide. Curr Pharm Des 2004;10:3331–48. [PubMed: 15544519]
3. Chiou GCXR. Effects of some natural flavonoids on retinal function recovery after ischemic insult in the rat. J of ocular Pharmacol and Therap 2004;20:107–113.
4. Garg A, Garg S, Zaneveld LJ, Singla AK. Chemistry and pharmacology of the Citrus bioflavonoid hesperidin. Phytother Res 2001;15:655–69. [PubMed: 11746857]
5. Beiler JM, Martin GJ. Inhibition of hyaluronidase action by derivatives of hesperidin. J of Biolog chem 1948;174:31–34.
6. Zhang J, Stanley RA, Melton LD, Skinner MA. Inhibition of lipid oxidation by phenolic antioxidants in relation to their physicochemical properties. Pharmacologyonline 2007;1:180–189.
7. Hirata A, Murakami Y, Shoji M, Kadoma Y, Fujisawa S. Kinetics of radical-scavenging activity of hesperetin and hesperidin and their inhibitory activity on COX-2 expression. Anticancer Res 2005;25:3367–74. [PubMed: 16101151]
8. Ayalasomayajula SP, Amrite AC, Kompella UB. Inhibition of cyclooxygenase-2, but not cyclooxygenase-1, reduces prostaglandin E2 secretion from diabetic rat retinas. Eur J Pharmacol 2004;498:275–8. [PubMed: 15364005]
9. Galati EM, Monforte MT, Kirjavainen S, Forestieri AM, Trovato A, Tripodo MM. Biological effects of hesperidin, a citrus flavonoid. (Note I): antiinflammatory and analgesic activity. Farmaco 1994;40:709–12. [PubMed: 7832973]
10. Monforte MT, Trovato A, Kirjavainen S, Forestieri AM, Galati EM, Lo Curto RB. Biological effects of hesperidin, a Citrus flavonoid. (note II): hypolipidemic activity on experimental hypercholesterolemia in rat. Farmaco 1995;50:595–9. [PubMed: 7495469]

11. Galati EM, Trovato A, Kirjavainen S, Forestieri AM, Rossitto A, Monforte MT. Biological effects of hesperidin, a Citrus flavonoid. (Note III): antihypertensive and diuretic activity in rat. Farmaco 1996;51:219–21. [PubMed: 8688145]
12. Tanaka T, Makita H, Ohnishi M, Mori H, Satoh K, Hara A, Sumida T, Fukutani K, Tanaka T, Ogawa H. Chemoprevention of 4-nitroquinoline 1-oxide-induced oral carcinogenesis in rats by flavonoids diosmin and hesperidin, each alone and in combination. Cancer Res 1997;57:246–52. [PubMed: 9000563]
13. Tanaka T, Makita H, Kawabata K, Mori H, Kakumoto M, Satoh K, Hara A, Sumida T, Tanaka T, Ogawa H. Chemoprevention of azoxymethane-induced rat colon carcinogenesis by the naturally occurring flavonoids, diosmin and hesperidin. Carcinogenesis 1997;18:957–65. [PubMed: 9163681]
14. Ameer B, Weintraub RA, Johnson JV, Yost RA, Rouseff RL. Flavanone absorption after naringin, hesperidin, and citrus administration. Clin Pharmacol Ther 1996;60:34–40. [PubMed: 8689809]
15. Gil-Izquierdo A, Gil MI, Tomas-Barberan FA, Ferreres F. Influence of industrial processing on orange juice flavanone solubility and transformation to chalcones under gastrointestinal conditions. J Agric Food Chem 2003;51:3024–8. [PubMed: 12720386]
16. Tsai TH, Liu MC. Determination of extracellular hesperidin in blood and bile of anaesthetized rats by microdialysis with high-performance liquid chromatography: a pharmacokinetic application. J Chromatogr B Analyt Technol Biomed Life Sci 2004;806:161–6.
17. Mitsunaga Y, Takanaga H, Matsuo H, Naito M, Tsuruo T, Ohtani H, Sawada Y. Effect of bioflavonoids on vincristine transport across blood-brain barrier. Eur J Pharmacol 2000;395:193–201. [PubMed: 10812049]
18. Ofer M, Wolffram S, Koggel A, Spahn-Langguth H, Langguth P. Modulation of drug transport by selected flavonoids: Involvement of P-gp and OCT? Eur J Pharm Sci 2005;25:263–71. [PubMed: 15911222]
19. Breinholt VM, Offord EA, Brouwer C, Nielsen SE, Brosen K, Friedberg T. In vitro investigation of cytochrome P450-mediated metabolism of dietary flavonoids. Food Chem Toxicol 2002;40:609–16. [PubMed: 11955666]
20. Kobayashi S, Tanabe S, Sugiyama M, Konishi Y. Transepithelial transport of hesperetin and hesperidin in intestinal Caco-2 cell monolayers. Biochim Biophys Acta 2008;1778:33–41. [PubMed: 18021752]
21. Serra H, Mendes T, Bronze MR, Simplicio AL. Prediction of intestinal absorption and metabolism of pharmacologically active flavones and flavanones. Bioorg Med Chem. 2008
22. Manach C, Morand C, Gil-Izquierdo A, Bouteloup-Demange C, Remesy C. Bioavailability in humans of the flavanones hesperidin and narirutin after the ingestion of two doses of orange juice. Eur J Clin Nutr 2003;57:235–42. [PubMed: 12571654]
23. Mitra, AK.; Macha, S.; Hughes, PM. Ophthalmic drug delivery systems. Marcel Dekker; 2003.
24. Bradford MM. A rapid and sensitive method for the quantitation of microgram quantities of protein utilizing the principle of protein-dye binding. Anal Biochem 1976;72:248–54. [PubMed: 942051]
25. Holekamp NM, Thomas MA, Pearson A. The safety profile of long-term, high-dose intraocular corticosteroid delivery. Am J Ophthalmol 2005;139:421–8. [PubMed: 15767049]
26. Jansen T, Xhonneux B, Mesens J, Borgers M. Beta-cyclodextrins as vehicles in eye-drop formulations: an evaluation of their effects on rabbit corneal epithelium. Lens Eye Toxic Res 1990;7:459–68. [PubMed: 2100172]
27. Saarinen-Savolainen P, Jarvinen T, Araki-Sasaki K, Watanabe H, Urtti A. Evaluation of cytotoxicity of various ophthalmic drugs, eye drop excipients and cyclodextrins in an immortalized human corneal epithelial cell line. Pharm Res 1998;15:1275–80. [PubMed: 9706061]
28. Loftssona T, Jarvinen T. Cyclodextrins in ophthalmic drug delivery. Adv Drug Deliv Rev 1999;36:59–79. [PubMed: 10837709]
29. Tommasini S, Calabro ML, Stancanelli R, Donato P, Costa C, Catania S, Villari V, Ficarra P, Ficarra R. The inclusion complexes of hesperetin and its 7-rhamnoglucoside with (2-hydroxypropyl)-beta-cyclodextrin. J Pharm Biomed Anal 2005;39:572–80. [PubMed: 15985355]
30. Wilcox DK. Extracellular release of acid hydrolases from cultured retinal pigmented epithelium. Invest Ophthalmol Vis Sci 1987;28:76–82. [PubMed: 3100474]

31. Adler AJ. Selective presence of acid hydrolases in the interphotoreceptor matrix. Exp Eye Res 1989;49:1067–77. [PubMed: 2612585]
32. Mannermaa E, Vellonen KS, Urtti A. Drug transport in corneal epithelium and blood-retina barrier: emerging role of transporters in ocular pharmacokinetics. Adv Drug Deliv Rev 2006;58:1136–63. [PubMed: 17081648]
33. Marshall WS, Klyce SD. Cellular and paracellular pathway resistances in the “tight” Cl- -secreting epithelium of rabbit cornea. J Membr Biol 1983;73:275–82. [PubMed: 6864779]
34. Prausnitz MR, Noonan JS. Permeability of cornea, sclera, and conjunctiva: a literature analysis for drug delivery to the eye. J Pharm Sci 1998;87:1479–88. [PubMed: 10189253]
35. Kansara V, Hao Y, Mitra AK. Dipeptide monoester ganciclovir prodrugs for transscleral drug delivery: targeting the oligopeptide transporter on rabbit retina. J Ocul Pharmacol Ther 2007;23:321–34. [PubMed: 17803430]
36. Majumdar S, Hippalgaonkar K, Repka MA. Effect of chitosan, benzalkonium chloride and ethylenediaminetetraacetic acid on permeation of acyclovir across isolated rabbit cornea. Int J Pharm 2008;348:175–8. [PubMed: 17897799]
37. Majumdar S, Nashed YE, Patel K, Jain R, Itahashi M, Neumann DM, Hill JM, Mitra AK. Dipeptide monoester ganciclovir prodrugs for treating HSV-1-induced corneal epithelial and stromal keratitis: in vitro and in vivo evaluations. J Ocul Pharmacol Ther 2005;21:463–74. [PubMed: 16386088]

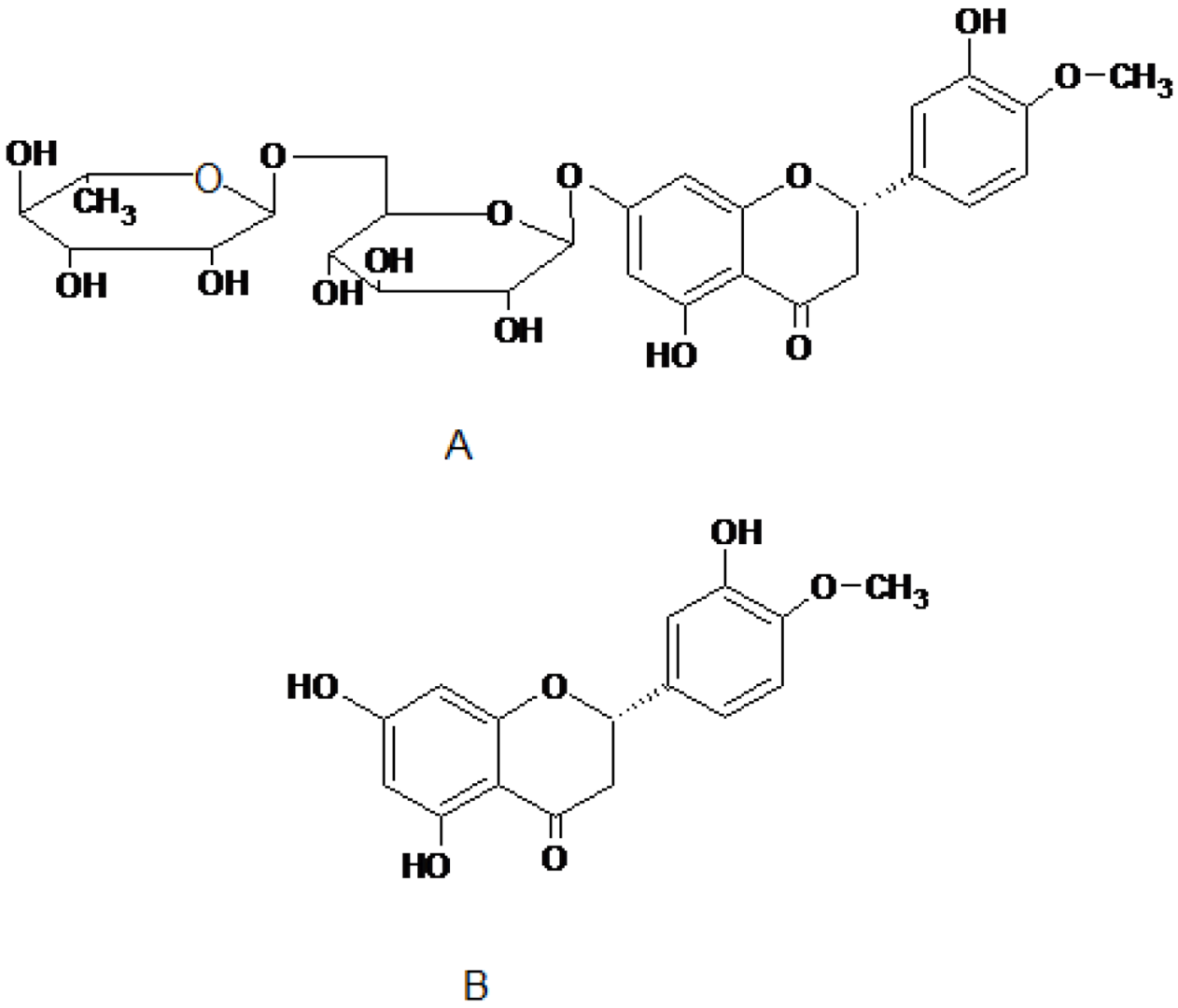

Figure 1.
A and B represents chemical structure of hesperidin (hesperetin –7-rhamnoglucoside) and hesperetin (3′, 5, 7-trihydroxy-4′-methoxy flavanone), respectively.

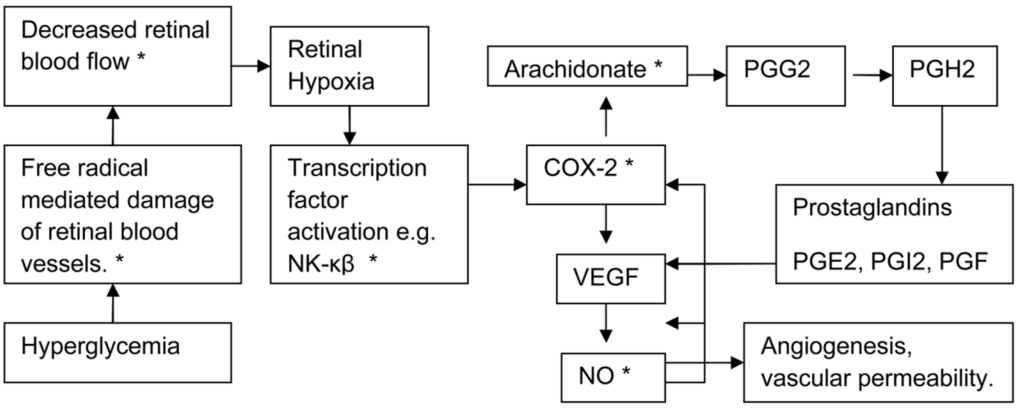

Figure 2.
Schematic representation of some of the currently identified pathways involved in the development and progression of diabetic retinopathy and macular degeneration. * Indicates pathways which hesperidin and hesperetin can potentially inhibit.

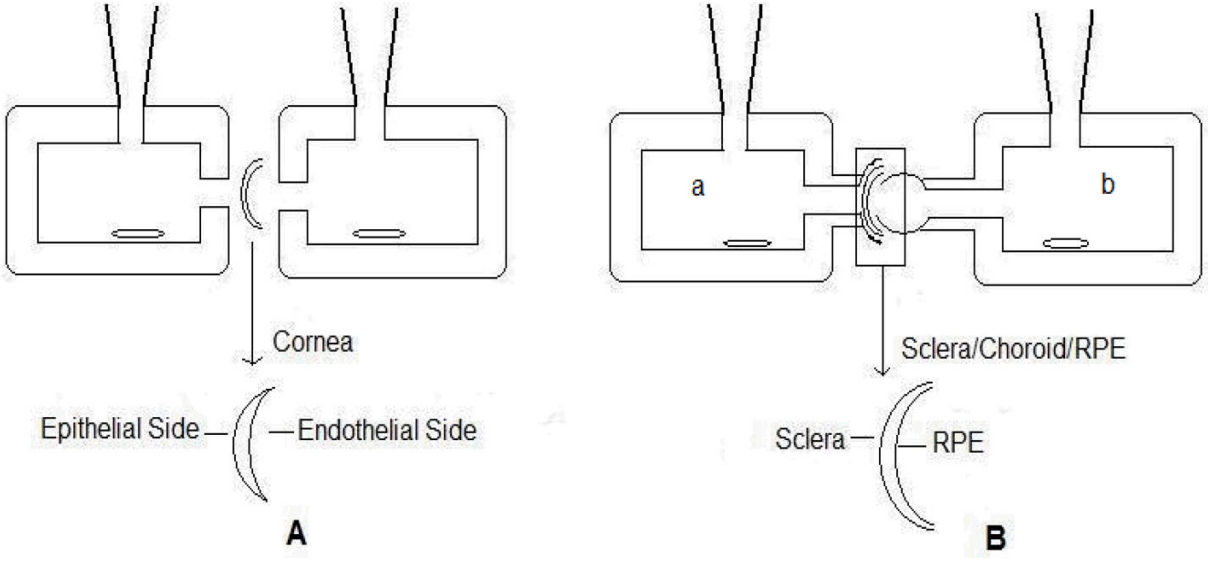

Figure 3.
Illustration depicting mounting of ocular tissue on regular side-bi-side diffusion cells (A) and on Valia-Chein Side-bi-Side diffusion cells (B)

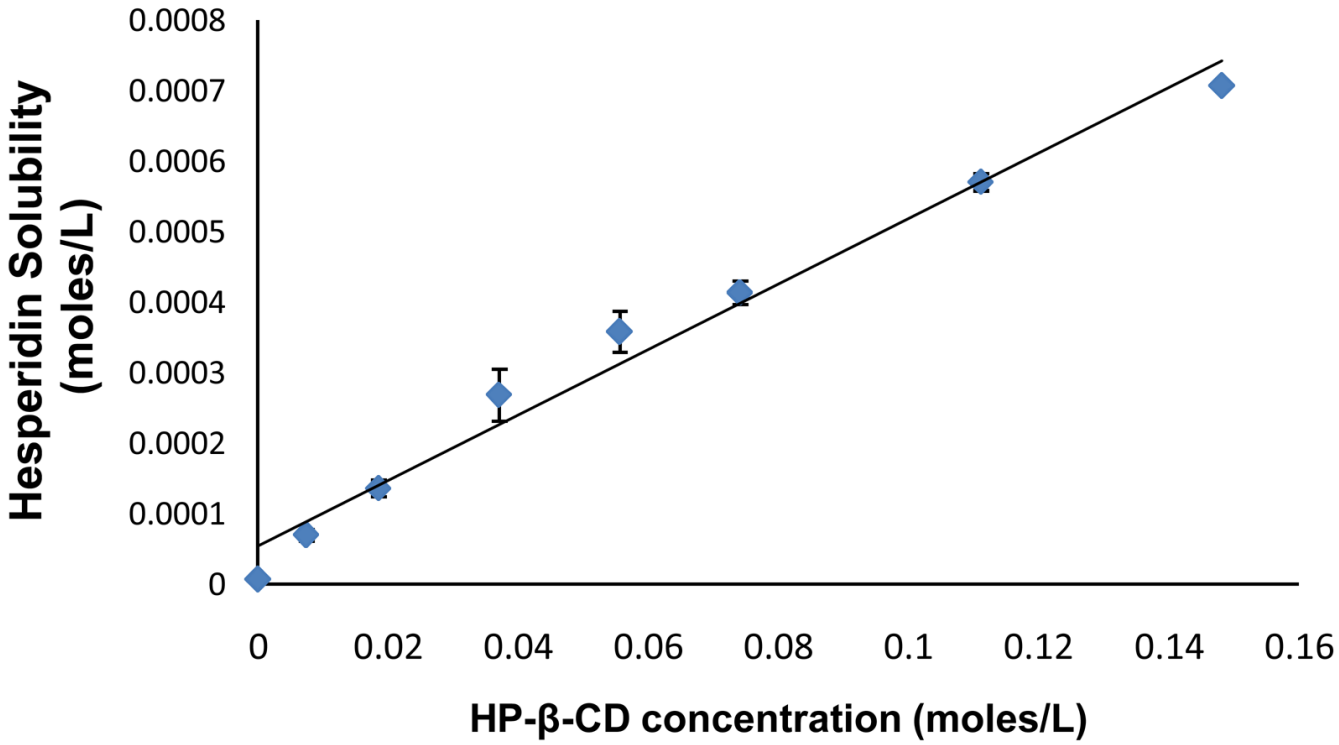

Figure 4.
Phase solubility of hesperidin in the presence of HP-β-CD, at 25°C, following 24h equilibration. Values are expressed as mean ± SD (n=3).

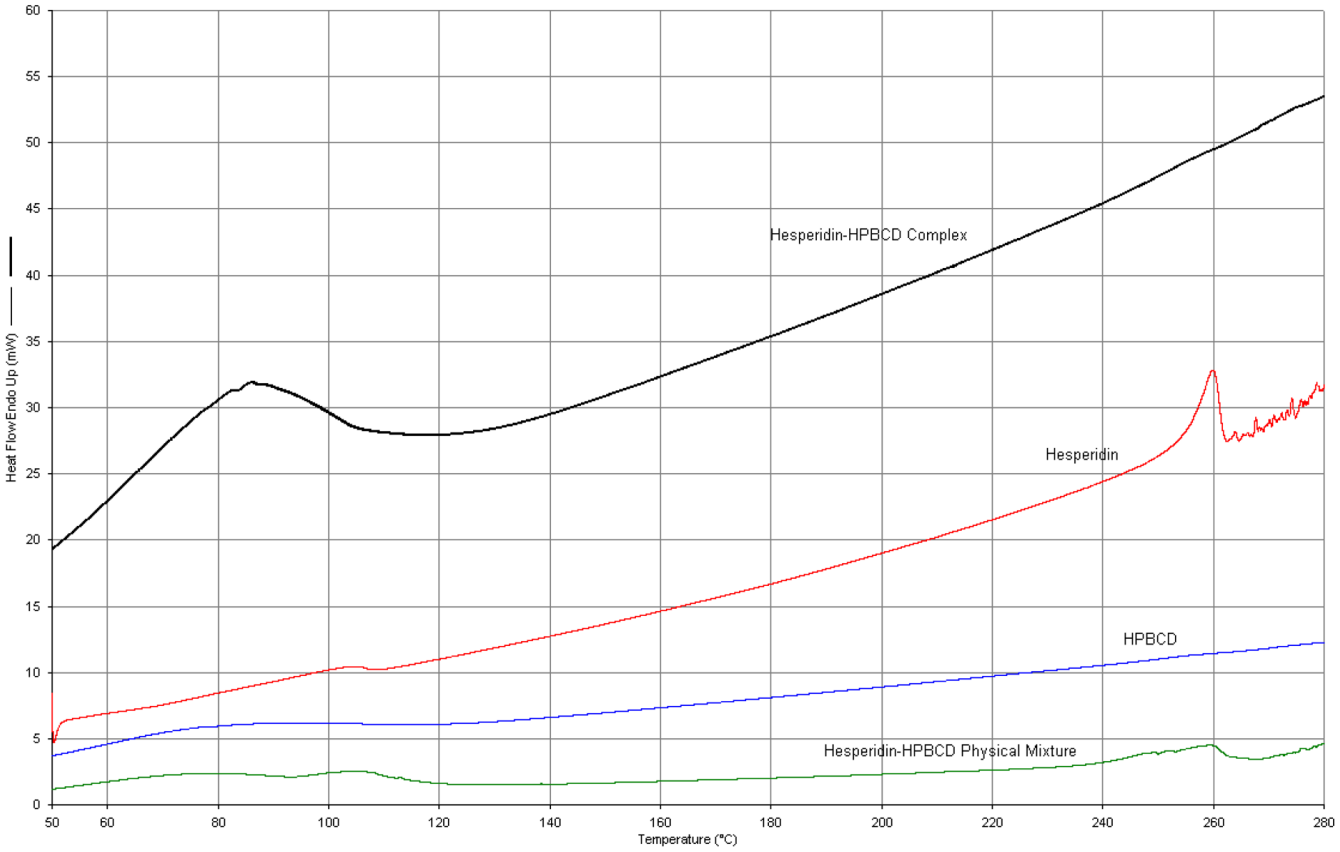

Figure 5.
DSC thermograms of the pure hesperidin and HP-β-CD, physical mixture of hesperidin and HP-β-CD (1:1 molar ratio) and the complex.

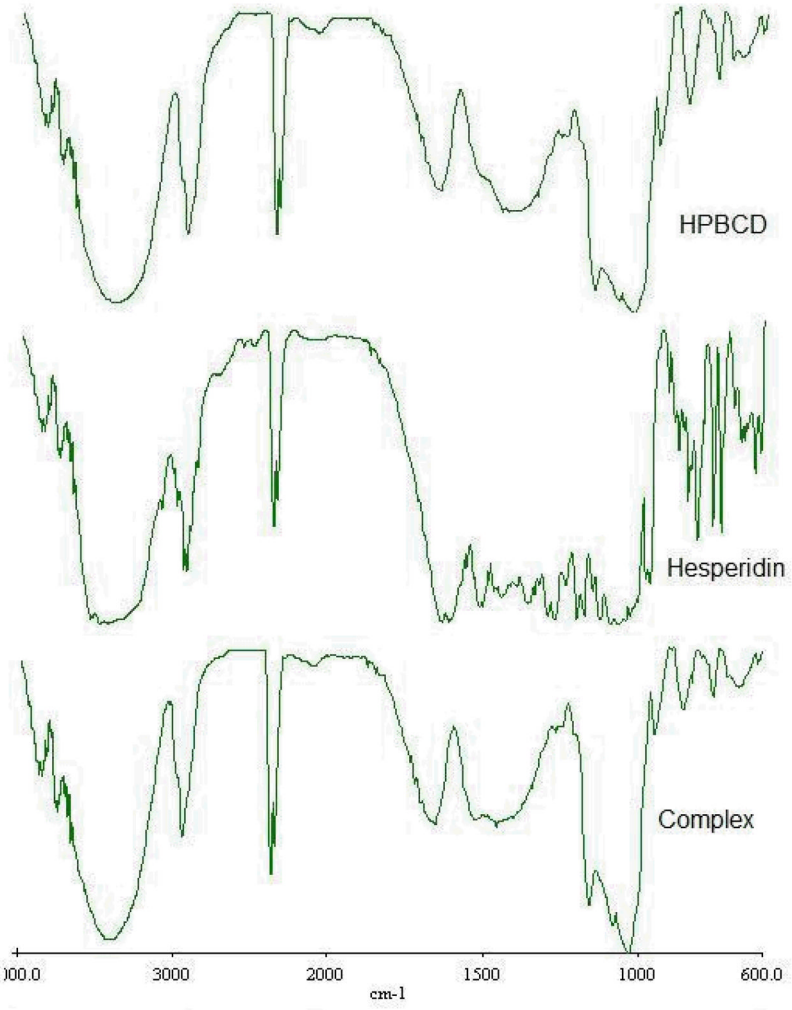

Figure 6.
FTIR spectra of the HP-β-CD, hesperidin and the complex.

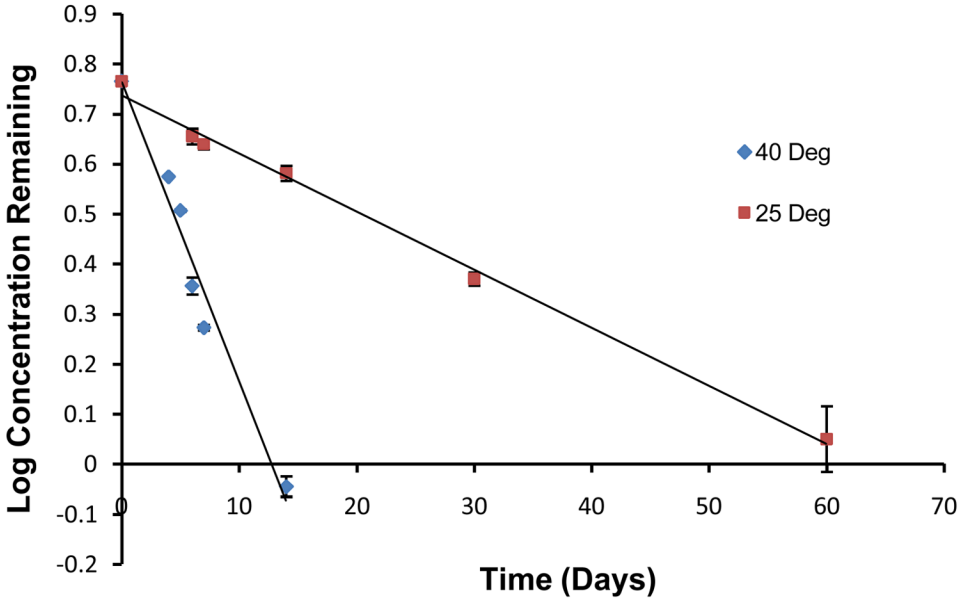

Figure 7.
Stability of hesperidin in pH 9 buffer at 25 and 40°C. Values are expressed as mean ± SD (n=3).

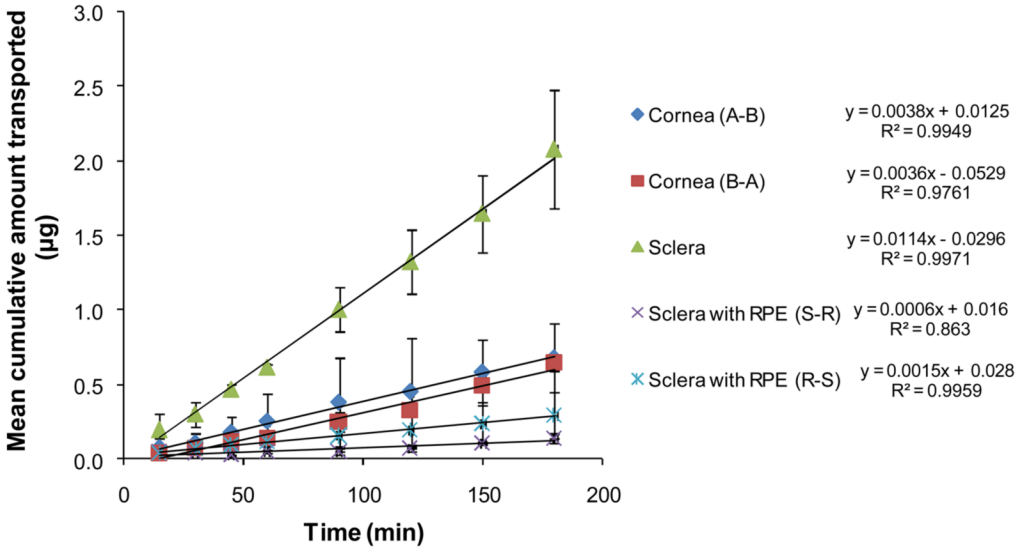

Figure 8.
Mean cumulative amount of hesperidin transported across ocular tissues as a function of time. Values are expressed as mean ± SD (n=4).

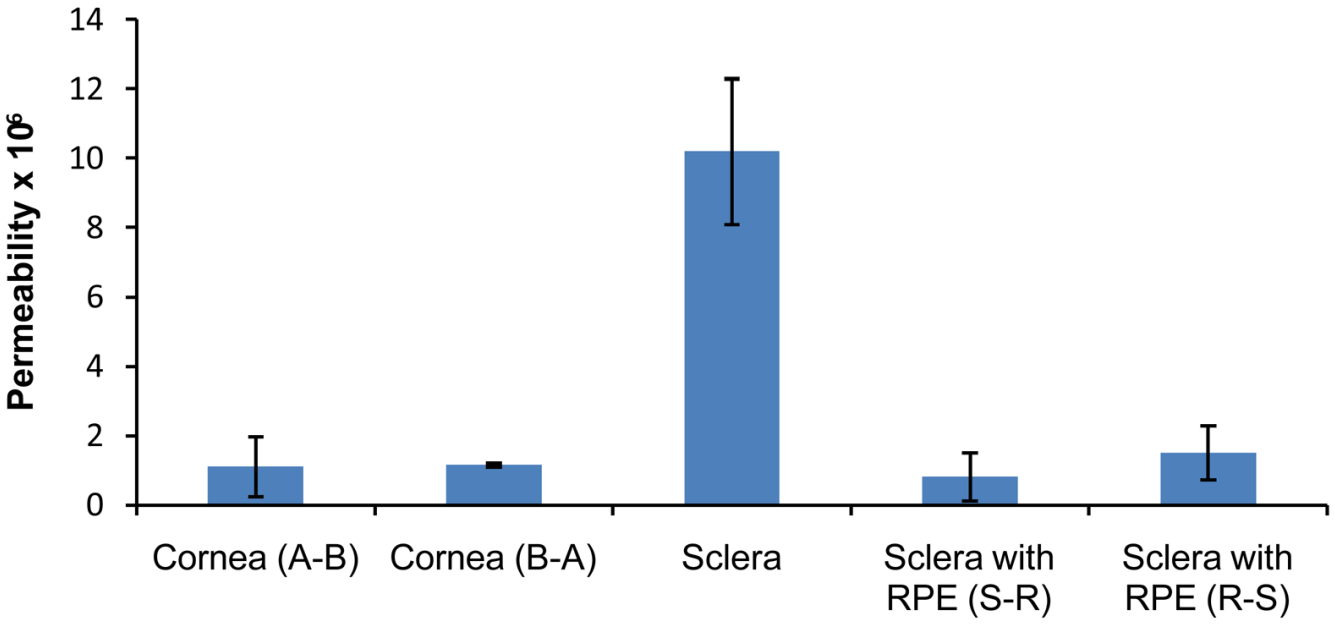

Figure 9.
Permeability (cm/s) of hesperidin across various ocular tissues. A-B denotes permeation in the apical to basolateral direction. S-R and R-S denotes permeation in the sclera to RPE direction and RPE to sclera direction. Values are expressed as mean ±SD (n=4).

Table I

Solubility of hesperidin as a function of pH (200 mM buffer concentration) and in water. The solubility studies were carried out at 25°C for a period of 24h. Values are expressed as mean ± SD (n=3).

pH	Saturation Solubility (μg/mL)
1.21	4.15 ± 0.34
3.11	8.44 ± 0.47
5.12	5.96 ± 1.92
7.48	5.26 ± 0.31
9.11	8.93 ± 0.73
Water	4.93 ± 0.99

Table II

Aqueous solubility of hesperidin (25°C, 24h equilibration) in the presence of various concentrations of HP-β-CD. Values are expressed as mean ± SD (n=3)

Concentration of HP-β-CD (%w/v)	Hesperidin Solubility (μg/mL)	Fold Increase in solubility
0	4.95 ± 0.99	
1	42.97 ± 4.28	9
2.5	83.34 ± 6.34	18
5	169.90 ± 25.36	37
7.5	219.03 ± 15.62	48
10	252.77 ± 8.81	55
15	348.55 ± 5.28	76
20	431.97 ± 0.43	95